

# Differential Hydration Thermodynamics of Stereoisomeric DNA–Benzo[*a*]pyrene Adducts Derived from Diol Epoxide Enantiomers with Different Tumorigenic Potentials

Luis A. Marky,<sup>\*,†</sup> Dionisios Rentzeperis,<sup>†,||</sup> Nataly P. Luneva,<sup>†,‡</sup> Monique Cosman,<sup>†,‡</sup> Nicholas E. Geacintov,<sup>†</sup> and Donald W. Kupke<sup>§</sup>

Contribution from the Department of Chemistry, New York University, New York, New York 10003, and Department of Biochemistry, University of Virginia, Charlottesville, Virginia 22908

Received November 17, 1995<sup>⊗</sup>

**Abstract:** A combination of UV spectroscopy, calorimetry, and density techniques were used to characterize the thermodynamics of complexes with covalently bound hydrophobic pyrenyl residues in the minor groove of DNA undecamer duplexes. The control duplex d(CCATCG\*CTACC)/d(GGTAGCGATGG) and two adduct duplexes in which the chiral (+)-*anti*-BPDE and (–)-*anti*-BPDE (the 7*R*,8*S*,9*S*,10*R*- and 7*S*,8*R*,9*R*,10*S*-enantiomers of 7*R*,8*t*-dihydroxy-9*t*,10*t*-epoxy-7,8,9,10-tetrahydrobenzo[*a*]pyrene) had been reacted covalently with the exocyclic amino group of the guanine residue G\* were studied (designated as the (+)- and (–)-BPDE duplexes, respectively). Both of the BPDE-modified DNA duplexes exhibit lower helix-coil transition temperatures than the control duplex. The complete thermodynamic profiles ( $\Delta V$ ,  $\Delta H$ ,  $\Delta G$ ,  $\Delta S$ , and  $\Delta n_{\text{Na}^+}$ ) for the formation of each duplex were determined at 20 °C. Duplex formation is primarily enthalpy driven, and is accompanied by an uptake of both counterions and water molecules (negative  $\Delta V$ ). Relative to the unmodified duplex, the differential thermodynamic profiles of each covalent adduct duplex reveal an enthalpy–entropy compensation; the  $\Delta\Delta V$  value is only marginally smaller for the (–)-BPDE–DNA than for the unmodified duplex, but the uptake of water is nearly 50% greater for the (+)-BPDE duplex. Correlation of the thermodynamic data with the known NMR solution conformations of the BPDE–DNA complexes (de los Santos et al. *Biochemistry* 1992, 31, 5245) suggests that these differential thermodynamic parameters, together with the similar values for the uptake of counterions, correspond to a differential hydration of the BPDE residues that are exposed to solvent while in the minor groove of B-DNA. The formation of the (+)-BPDE duplex results in a greater immobilization of structural water than in the case of the (–)-BPDE duplex; these results suggest that the bent conformation at the lesion site apparently gives rise to an enhanced exposure of the hydrophobic polycyclic aromatic moiety of the covalently bound BPDE residue to the aqueous solvent.

## Introduction

Alterations in the characteristics and structural properties of DNA due to chemical carcinogens are widely believed to be the critical factors which give rise to mutations and the initiation of tumorigenesis.<sup>1–4</sup> *In vivo*, polycyclic aromatic hydrocarbons (PAH) are metabolized to highly reactive diol epoxide derivatives that bind covalently to DNA. Their biological activities are markedly dependent on their chemical structures and stereochemical configurations.<sup>3–5</sup> Benzo[*a*]pyrene, one of the most widely studied PAH compounds, is metabolized *in vivo* to highly reactive stereoisomeric bay region 7,8-dihydroxy-9,10-epoxide derivatives. Particularly striking are the differences in the tumorigenic and mutagenic activities of the chiral (7*R*,8*S*-

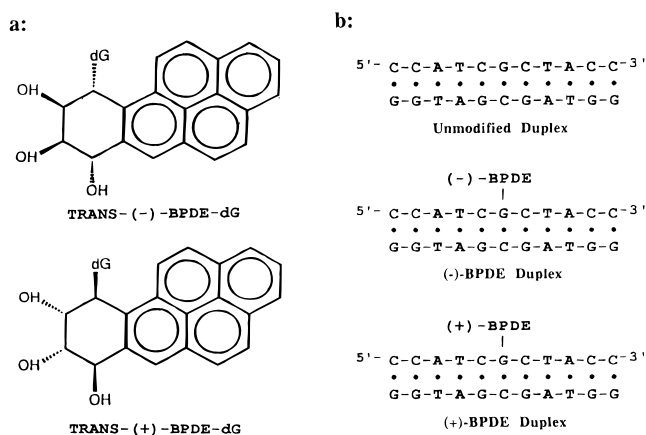


**Figure 1.** (a) Structure of the *trans*-(-)- and *trans*-(+)-benzo[*a*]pyrene–N<sup>2</sup>-dG adducts. (b) Structure of duplexes.

dihydroxy-(9*S*,10*R*)-epoxy-7,8,9,10-tetrahydrobenzo[*a*]pyrene ((+)-*anti*-BPDE) and 7*S*,8*R*,9*R*,10*S*-enantiomer ((–)-*anti*-BPDE) (Figure 1a). While (+)-*anti*-BPDE is strongly tumorigenic, (–)-*anti*-BPDE is not.<sup>5</sup> In mammalian cells, (+)-*anti*-BPDE is more mutagenic than (–)-*anti*-BPDE,<sup>6,7</sup> while in bacterial cells, the relative mutagenicities are strain-depend-

(6) Wood, A. W.; Chang, R. L.; Levin, W.; Yagi, H.; Thakker, D. R.; Jerina, D. M.; Conney, A. H. *Biochem. Biophys. Res. Commun.* 1977, 77, 1389.

(7) Brookes, P.; Osborne, M. R. *Carcinogenesis* 1982, 3, 1223.

\* To whom correspondence should be addressed.

† New York University.

|| Present address: Department of Biology, Massachusetts Institute of Technology, Boston, MA 02130.

‡ Present address: Russian Academy of Sciences, Chernogolovka, Russia 142432.

§ Present address: Lawrence Livermore National Laboratory, Livermore, CA 94551.

⊗ University of Virginia.

⊙ Abstract published in *Advance ACS Abstracts*, April 1, 1996.

(1) Ashurst, S. W.; Cohen, G. M.; Nesnow, S.; DiGiovanni, J.; Slaga, T. J. *Cancer Res.* 1983, 43, 1024.

(2) Weinstein, I. B. *Cancer Res.* 1988, 48, 4135.

(3) Singer, B.; Grunberger, D. In *Molecular Biology of Mutagens and Carcinogens*; Plenum Press: New York, 1983.

(4) Singer, B.; Essigman, J. M. *Carcinogenesis* 1991, 12, 949.

(5) Conney, A. H. *Cancer Res.* 1982, 42, 4875.

ent.<sup>6,8,9</sup> These differences have been attributed to the characteristics and conformations of the covalent adducts derived from the binding of these two enantiomers to cellular DNA, and differences in the processing of these lesions by cellular enzyme systems.<sup>7,9</sup>

The conformations of the covalent adducts derived from the binding of (+)- and (–)-BPDE to DNA and other nucleic acids have been extensively studied by spectroscopic methods.<sup>10–12</sup> Recently, techniques have been devised to synthesize sufficiently large quantities of stereospecific and site-specific (+)- and (–)-BPDE–deoxyoligonucleotide adducts<sup>13</sup> for spectroscopic,<sup>14</sup> thermodynamic,<sup>15</sup> and high-resolution NMR studies.<sup>16,17</sup> The major adduct formed with DNA involves trans addition of *anti*-BPDE (C10 position) to N<sup>2</sup> of guanine as shown earlier.<sup>7,18–21</sup> On the basis of optical spectroscopic studies, it was suggested that in adducts derived from the binding of either (+)-*anti*-BPDE or (–)-*anti*-BPDE by trans-addition to N<sup>2</sup>-Guanine in an 11-mer oligonucleotides containing one single guanine residue (duplexes of these modified 11-mers with their natural complementary strands are designated here as (+)- and (–)-BPDE–DNA, respectively), the pyrenyl residues are exposed partially to the aqueous solvent environment;<sup>14</sup> detailed NMR studies of the solution structures of the (–)-BPDE duplex<sup>17</sup> and the (+)-BPDE duplex<sup>16,17</sup> have shown unambiguously that the benzo[*a*]pyrene ring lies in the minor groove of the DNA duplex. One face of the adduct makes extensive van der Waals contacts with the sugar phosphate backbone of the complementary strand while the other face is exposed to aqueous solvent. The chirality of the BPDE enantiomers manifests itself in striking opposite orientations of the pyrenyl residues in the adducts; in the (–)-BPDE–DNA adduct the pyrenyl residue is oriented toward the 3' end of the modified strand, while in the (+)-BPDE–DNA adduct it is oriented toward the 5' end.<sup>16,17</sup> Another striking difference between these two isomeric BPDE–DNA duplexes is that the gel electrophoretic mobilities of the (+)-BPDE–DNA duplexes are significantly slower than those of the (–)-BPDE–DNA duplexes.<sup>22,23</sup> These observations suggest that the

(+)-BPDE–N<sup>2</sup>-dG lesions are associated with greater degrees of bending or flexibility than the (–)-BPDE–N<sup>2</sup>-dG lesions.

The physical characteristics of these two stereoisomeric adducts have long been of interest<sup>7,9,13–14,16–17,22</sup> for gaining an understanding of the chemical basis of the differences in their biological activities of the two chiral *anti*-BPDE enantiomers associated with the formation of these DNA adducts.<sup>5–9</sup> The availability of conformational information,<sup>13–14,22</sup> especially the detailed NMR structural features,<sup>16,17</sup> has motivated us to compare the thermodynamic characteristics of these (+)-BPDE- and (–)-BPDE-modified oligomer duplexes.

Thermodynamic investigations of the helix–coil transition of oligonucleotides of defined base sequences have greatly enhanced our understanding of the conformational transitions of nucleic acid molecules.<sup>24,25</sup> Preliminary studies of UV melting curves at low oligonucleotide concentrations (<10 μM strand concentration) have shown that the BPDE residues tend to destabilize the oligonucleotide duplexes.<sup>14</sup> In the present work, we used density and isothermal titration calorimetry techniques to measure directly the volume change and enthalpy of formation, Δ*H*<sub>ITC</sub>, of each duplex (shown in Figure 1b) from the mixing of their complementary strands. Duplex formation is enthalpy driven, and is accompanied by an uptake of water molecules (negative Δ*V*). The Δ*V* value for the (+)-BPDE duplex of –209 mL/mol is larger than the value of –136 mL/mol for the (–)-BPDE duplex, which is similar in magnitude to the value of –144 mL/mol for the unmodified duplex. Complementary measurements of the helix–coil transition of each duplex, using differential scanning calorimetry and UV spectroscopy melting techniques, allow us to determine with proper extrapolations additional thermodynamic parameters (Δ*G*, Δ*S*, and Δ*n*<sub>Na<sup>+</sup></sub>) of duplex formation at 20 °C. Correlation of the resulting and complete thermodynamic data with the known structural characteristics of the BPDE–DNA complexes suggests that these thermodynamic parameters, together with the similar values for the uptake of counterions, correspond to a difference in the hydration of the hydrophobic BPDE residues positioned in the minor groove of the (+)- and (–)-BPDE–DNA adducts. This suggest that the formation of the (+)-BPDE-duplexes results in additional immobilization of structural water; the bent conformation at the lesion site in the (+)-BPDE–DNA duplex is consistent with a greater exposure of the hydrophobic atomic groups of the covalently bound moieties to the aqueous solvent molecules.

## Materials and Methods

**Materials.** The racemic BPDE (7*r*,8*t*-dihydroxy-9*r*,10*r*-epoxy-7,8,9,10-tetrahydrobenzo[*a*]pyrene, called often *anti*-BPDE or BPDE 2) was purchased from the National Cancer Institute Chemical Carcinogen Reference Standard Repository (Midwest Research Institute, Kansas City, MO). The deoxyoligonucleotides 5'-CCATCGCTACC-3' and 5'-GGTAGCGATGG-3' were synthesized employing a Biosearch Cyclone DNA synthesizer (Biosearch, Inc., San Rafael, CA), using standard phosphoramidite chemistry following procedures described previously,<sup>26</sup> purified by HPLC methods, and desalted on a Sephadex G-10 exclusion chromatography column.

The oligonucleotide 5'-CCATCGCTACC-3' was reacted with racemic BPDE in aqueous buffer systems, and the two oligonucleotides in

(8) Burgess, J. A.; Stevens, C. W.; Fahl, W. E. *Cancer Res.* **1985**, *45*, 4257.

(9) Stevens, C. W.; Bouck, N.; Burgess, J. A.; Fahl, W. E. *Mutation Res.* **1985**, *152*, 5.

(10) Harvey, R. G.; Geacintov, N. E. *Acc. Chem. Res.* **1987**, *21*, 66.

(11) Geacintov, N. E. In *Polycyclic Aromatic Hydrocarbon Carcinogenesis: Structure Activity Relationships*; Yang, S. K., Silverman, B. D., Eds.; CRC Press: Boca Raton, FL, 1988; Vol. II, pp 181–206.

(12) Grädslund, A.; Jernström, B. *Q. Rev. Biophys.* **1989**, *22*, 1.

(13) Cosman, M.; Ibanez, V.; Geacintov, N. E.; Harvey, R. G. *Carcinogenesis* **1990**, *11*, 1667.

(14) Geacintov, N. E.; Cosman, M.; Mao, B.; Alfano, A.; Ibanez, V.; Harvey, R. G. *Carcinogenesis* **1991**, *12*, 2099.

(15) (a) Cosman, M.; Geacintov, N. E.; Amin, S. In *Polycyclic Aromatic Compounds: Synthesis, Properties, Analytical Measurement, Occurrence and Biological Effects*; Garrigues P., Lamotte M., Eds.; Gordon and Breach Science Publishers: France, 1991; Vol. 3, pp 1151–1158. (b) Ya, N.-Q.; Smirnov, S.; Cosman, M.; Bhanot, S.; Ibanez, V.; Geacintov, N. E. In *Structural Biology: The State of the Art. Proceedings of the 8th Constaion*; Sarma, R. H., Sarma, M. H. Adenine Press: Schenectady, NY, 1994; Vol. 2, pp 349–366.

(16) Cosman, M.; de los Santos, C.; Fiala, R.; Hingerty, B. E.; Singh, S. B.; Ibanez, V.; Margulis, L. A.; Live, D.; Geacintov, N. E.; Broyde, S.; Patel, D. J. *Proc. Natl. Acad. Sci. U.S.A.* **1992**, *89*, 1914.

(17) De los Santos, C.; Cosman, M.; Hingerty, B. E.; Ibanez, V.; Margulis, L. A.; Geacintov, N. E.; Broyde, S.; Patel, D. J. *Biochemistry* **1992**, *31*, 5245.

(18) Weinstein, I. B.; Jeffrey, A. M.; Jettette, K. W.; Blobstein, S. H.; Harvey, R. G.; Harris, C.; Autrup, H.; Kasai, H.; Nakanishi, K. *Science* **1976**, *193*, 592.

(19) Koreeda, M.; Moore, P. D.; Wislocki, P. G.; Levin, W.; Conney, A. H.; Yagi, H.; Jerina, D. M. *Science* **1978**, *199*, 778.

(20) Meehan, T.; Straub, K. *Nature* **1979**, *277*, 410.

(21) Cheng, S. C.; Hilton, B. D.; Roman, J. M.; Dipple, A. *Chem. Res. Toxicol.* **1989**, *2*, 334.

(22) Mao, B. Ph.D. Dissertation, New York University, 1994.

(23) (a) Xu, R.; Mao, B.; Xu, J.; Li, B.; Birke, S.; Swenberg, C. E.; Geacintov, N. E. *Nucleic Acids Res.* **1995**, *23*, 2314–2319. (b) Xu, R.; Mao, B.; Amin, S.; Geacintov, N. E. In preparation.

(24) Breslauer, K. J.; Frank, R.; Blöcker, H.; Marky, L. A. *Proc. Natl. Acad. Sci. U.S.A.* **1986**, *83*, 3746.

(25) Freier, S. M.; Kierzek, R.; Jaeger, J. A.; Sugimoto, N.; Caruthers, M. H.; Neilson, T.; Turner, D. H. *Proc. Natl. Acad. Sci. U.S.A.* **1986**, *83*, 9373.

(26) Caruthers, M. H. In *Chemical and Enzymatic Synthesis of Gene Fragments*; Gassen, H. G., Lang, A., Eds.; Verlag Chemie: Weinheim, FRG, 1982; pp 71–79.

which the single guanine is modified at the exocyclic amino group ((+)- and (-)-*trans*-BPDE-N<sup>2</sup>-dG adducts, respectively) were separated from the reaction mixture, and characterized according to procedures fully described earlier.<sup>13,14</sup> Extinction coefficients of the unmodified oligomers in single strands at 260 nm were calculated for 25 °C using the tabulated values of the dimers and monomer bases<sup>27</sup> and estimated at high temperatures by extrapolation to 25 °C of the upper portions of the melting curves,<sup>28</sup> which correspond to the UV-temperature dependence of the absorbance of the single strands. A similar procedure was used for the modified oligomer strands, and a value of 4 mM<sup>-1</sup>·cm<sup>-1</sup> at 260 nm was used for the additional optical contribution of the BPDE moiety. The concentration of stock aqueous oligomer solutions was determined using the following extinction coefficients of strands at 260 nm and 80 °C, with all values given in mM<sup>-1</sup> cm<sup>-1</sup>: 98 (unmodified 11-mer 5'-CCATCGCTACC-3'), 103 and 101 (BPDE-modified 11-mers 5'-CCATCG(-)<sup>BPDE</sup>CTACC-3' and CCATCG(+)<sup>BPDE</sup>CTACC-3'), and 115 for the unmodified complementary strand 5'-GGTAGCGATGG-3'. Similar extinction coefficients (within 3%) were obtained by phosphate analysis.

Stock oligomer solutions were prepared by dissolving the dry and desalted oligomers in a buffer solution consisting of 20 mM sodium phosphate, 0.1 M NaCl, pH 7.0. The stoichiometries of each duplex were determined spectroscopically using the method of continuous variations in which one of the strands is mixed with the corresponding complementary strand while the total strand concentration is kept constant. All chemicals were reagent grade.

**Magnetic Suspension Densimetry.** The volume change,  $\Delta V$ , that accompanies the formation of each duplex was determined by measuring the density on weighed samples in a magnetic-suspension densimeter at 20 °C ( $\pm 0.001$ ).<sup>29</sup> The  $\Delta V$  value is calculated by measuring the mass and the equilibrium density of solutions before and after mixing; the observed change in volume,  $\Delta v$ , upon adding strand A to its complementary strand B to form a DNA duplex AB is given by:

$$\Delta v = m_{AB}/\rho_{AB} - (m_A/\rho_A + m_B/\rho_B) \quad (1)$$

where  $m$  is the mass in grams and  $\rho$  is the density of the solutions in grams per milliliter. The density of each sample is obtained by relating the measured voltage to the straight line calibration equation of voltage versus density of aqueous KCl solutions of known density and its precision is  $< 5 \times 10^{-6}$  g/mL. The concentration of each strand ranged from 2.9 to 3.9 mM in residues. The value of  $\Delta V$  is obtained after normalizing the  $\Delta v$  (in nanoliters) for the number of moles of the limiting strand. To make sure that the duplexes are formed completely, weighed duplex samples were heated to 50 °C and cooled to room temperature in tightly closed 0.4 mL polyethylene tubes to prevent evaporation.

**Titration Calorimetry.** The measurement of the heats of mixing a single strand with its corresponding complementary strand at 20 °C was carried out using the Omega titration calorimeter from Microcal Inc. (Northampton, MA).<sup>30</sup> Solutions of one strand were used to titrate the complementary strand to form each duplex. A 100- $\mu$ L syringe was used to inject the titrant; mixing was effected by stirring this syringe at 400 rpm. Typically 7–10 injections of 7  $\mu$ L each were performed in a single titration, and the concentration (in strands) of the oligomer in the syringe was  $\sim 20$  times higher than the concentration of the complementary strand in the reaction cell ( $\sim 5 \mu$ M). The reference cell was filled with distilled water and the instrument was calibrated by means of a known standard electrical pulse. The calorimetric titrations were designed to obtain primarily the enthalpy of formation of each duplex ( $\Delta H_{ITC}$ ) under unsaturating conditions and are obtained by averaging the heats of the initial 4 to 5 injections.

**Differential Scanning Calorimetry.** The total heat of the helix-coil transition of each duplex was measured directly with a Microcal MC-2 (Northampton, MA) differential scanning calorimeter (DSC). Typically, an oligomer solution with a concentration of 0.35–0.55 mM (in strands) versus buffer was scanned from 20 to 90 °C at a heating

**Table 1.** Isothermal Heat and Volume Change Measurements for the Formation of Each Duplex from Mixing Their Complementary Strands at 20 °C.

duplex	$\Delta H_{ITC}$ (kcal/mol)	$\Delta V$ (mL/mol)
unmodified	-82( $\pm 3$ )	-144( $\pm 10$ )
(-)-BPDE	-47( $\pm 2$ )	-136( $\pm 11$ )
(+)-BPDE	-49( $\pm 2$ )	-209( $\pm 14$ )

<sup>a</sup> Values determined in 20 mM sodium phosphate buffer, 0.1 M NaCl at pH 7.

rate of 0.75 °C min<sup>-1</sup> with 5 repetitions. A buffer versus buffer scan was subtracted from the sample scan and normalized for the heating rate, i.e., each data point was divided by the corresponding heating rate. The area of the resulting curve is proportional to the transition heat, which, when normalized for the number of moles, is equal to the transition enthalpy,  $\Delta H_{cal}$ . The instrument was calibrated with a standard electrical pulse. The analysis of the shape of the resulting heat capacity functions allows us to calculate model-dependent enthalpies,  $\Delta H_{vH}$ . Direct comparisons of  $\Delta H_{vH}$  with  $\Delta H_{cal}$  permit us to interpret the nature of the transition.<sup>31</sup>

**UV Melting Curves.** Absorbance versus temperature profiles for the oligomeric duplexes, at several strand concentrations and in buffer solutions containing 0 to 100 mM of NaCl, were measured at 260 nm with a thermoelectrically controlled Perkin-Elmer 552 spectrophotometer interfaced to a PC-XT computer for acquisition and analysis of experimental data. The temperature was scanned at a heating rate of 1 °C min<sup>-1</sup>. From these melting curves we extract the midpoint transition temperatures,  $T_m$ , and the van't Hoff transition enthalpies. These parameters were calculated using standard procedures reported previously,<sup>31</sup> and correspond to the usual two-state helix-coil approximation. From the  $T_m$ -salt dependence ( $T_m$  vs log [Na<sup>+</sup>] plots) together with the  $T_m$ 's and enthalpies obtained from DSC experiments, the amount of counterion release was estimated for each duplex.

## Results

**Overview of Experimental Approach.** In order to obtain complete thermodynamic profiles for the formation of BPDE-DNA adducts at 20 °C, and to correlate the resulting energetics with the molecular interactions observed in their solution structures, we first used magnetic-suspension densimetry and isothermal titration calorimetry to measure the volume change and heat of duplex formation (from the mixing of complementary strands), respectively. The additional  $\Delta G$  and  $\Delta S$  parameters are determined from the standard thermodynamic profiles of the helix-coil transition of each duplex. These are measured in DSC experiments and are temperature extrapolated from  $T_m$  to 20 °C and corrected for the contribution of disrupting base-base stacking interactions in the single strands at 20 °C. We also used UV melting techniques (in conjunction with DSC) both to measure the amount of counterion release and to test the applicability of two-state transitions, by comparison of van't Hoff enthalpies with the model-independent enthalpy ( $\Delta H_{cal}$ ).

**Formation of Each Duplex Is Accompanied by an Uptake of Water Molecules.** We have used a magnetic suspension densimeter to measure directly at 20 °C the change in volume associated with the formation of each duplex from mixing its complementary strands. The results are listed in Table 1 and correspond to an average of at least two determinations; in these experiments we used a slight excess of the complementary strand over the BPDE-modified strand to assure complete duplex formation. The negative  $\Delta V$  values in Table 1 indicate that the formation of each duplex is accompanied by an uptake of water molecules. The  $\Delta V$  term at constant temperature and pressure results from the net change in the molar volume of water, and is essentially the net change in compression of the water dipoles in response to the intermolecular solute-solute interactions. Thus, the observed  $\Delta V$  may be regarded as the

(27) Cantor, C. R.; Warshaw, M. M.; Shapiro, H. *Biopolymers* **1970**, *9*, 1059.

(28) Marky, L. A.; Blumenfeld, K. S.; Kozlowski, S.; Breslauer, K. J. *Biopolymers* **1983**, *22*, 1247.

(29) Gillies, G. T.; Kupke, D. W. *Rev. Sci. Instrum.* **1988**, *59*, 307.

(30) Wiseman, T.; Williston, S.; Brandts, J. F.; Lin, L. N. *Anal. Biochem.* **1989**, *179*, 131.

(31) Marky, L. A.; Breslauer, K. J. *Biopolymers* **1987**, *26*, 1601.

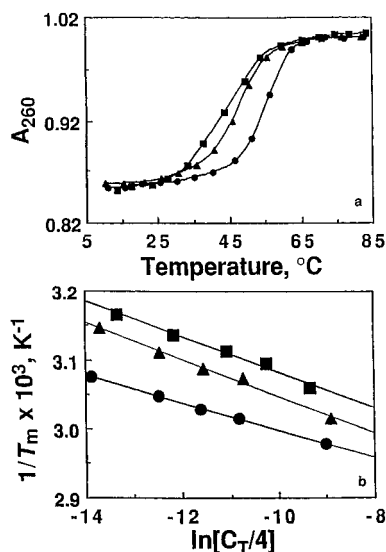


**Figure 2.** (a) Typical normalized optical melts at 260 nm in 20 mM NaPi buffer containing 0.1 M NaCl at pH 7 and at a fixed strand concentration of  $\sim 18 \mu\text{M}$ ; unmodified duplex ( $\bullet$ ), (-)-BPDE ( $\blacktriangle$ ), (+)-BPDE ( $\blacksquare$ ). (b) Dependence of the transition temperature on strand concentration (4–500  $\mu\text{M}$ ) for each oligomer duplex in the same buffer; symbols as above.

net change due to the thermodynamic hydration of the solute, i.e., its degree of hydration. The significant observation is that the uptake of water molecules for the unmodified duplex and the (-)-BPDE duplex is the same, within experimental error, while the uptake is about 50% larger for the (+)-BPDE duplex.

**Formation of Each Duplex Is Accompanied by Exothermic Enthalpy Changes.** In order to further characterize the thermodynamic characteristics of duplex formation, and to relate these to the measured values of  $\Delta V$ , we carried out titration calorimetric experiments at 20 °C, a temperature where duplexes are fully formed since the thermal melting points are significantly above this temperature (see below). The results of these measurements are shown in Table 1. The exothermic enthalpies for the formation of each duplex result from the balance of exothermic contributions (formation of base-pair stacks and/or uptake of water molecules), and endothermic contributions (such as disruption of base–base stacking interactions in the single strands); the uptake of counterions contributes little to the enthalpy of duplex formation.<sup>32,33</sup> The magnitudes of these enthalpies of formation depend on the nature of the duplex that is being formed, being more highly exothermic for the unmodified duplex and 41% less exothermic for each of the two modified duplexes. At 20 °C, this indicates a larger endothermic contribution of disrupting base-stacking interactions of the single strands containing the BPDE moiety, since all other contributions are similar for each duplex.

**UV Melting Curves.** Melting curves (Figure 2a) were measured by following the UV absorbance at 260 nm and total strand concentration ranging from 4 to 140  $\mu\text{M}$ ; hyperchromicities of  $\sim 16\%$  are observed at this wavelength of measurement with  $T_m$ 's in the following order of duplex stability: unmodified duplex > (-)-BPDE > (+)-BPDE; both observations are consistent with previous results.<sup>15b</sup> Figure 2b shows the typical linear dependence of  $1/T_m$  on  $\ln(C_T/4)$ , the data points at the highest concentration in each plot obtained from the DSC experiments. The relevant enthalpy data obtained from these experiments are presented in Table 2. The helix–coil

transition of each duplex is accompanied by an endothermic heat that corresponds primarily to the disruption of hydrogen bonding and base-pair stacking interactions.

**Differential Scanning Calorimetry and the Nature of the Transitions.** Typical excess heat capacity versus temperature profiles are presented in Figure 3. While the last four repetitive scans of each oligomer duplex were reproducible, the first showed typical deviations due to the conditioning of the DSC cells to temperature and to contact of solutions. Each transition shows negligible changes in the heat capacities between the initial and final states, and the area under these curves is proportional to the total endothermic heat ( $\Delta H_{\text{cal}}$ ) needed to disrupt these duplexes into single strands. The van't Hoff and calorimetric enthalpies measured from these curves are compared in Table 2. The  $\Delta H_{\text{cal}}$  value of 80.1 kcal mol<sup>-1</sup> for the unmodified duplex is in excellent agreement with the enthalpy of 85.3 kcal mol<sup>-1</sup>, estimated from nearest-neighbor parameters;<sup>24</sup> the small difference may be attributed to the use of 1 M NaCl in the latter determination. In the case of the modified duplexes relative to the unmodified undecameric duplex, we measured a decrease of 7.4 kcal mol<sup>-1</sup> in the enthalpy values for the (-)-BPDE duplex and a decrease of 16.6 kcal mol<sup>-1</sup> for the (+)-BPDE duplex. Comparison of the van't Hoff enthalpies ( $\Delta H_{\text{vH}}$ ), calculated from the shape of the DSC curves, with the transition enthalpies measured directly by differential scanning calorimetry, allows us to draw conclusions about the nature of these transitions.<sup>31</sup> At this salt concentration, we obtained  $\Delta H_{\text{vH}}/\Delta H_{\text{cal}}$  ratios of 1.12 for the unmodified duplex and 1.00 and 1.09 for the transitions of the (-)-BPDE and (+)-BPDE duplexes, respectively. Thus, all three duplexes melt according to a two-state transition model since these ratios are close to unity.<sup>31</sup> It should be emphasized that this simple analysis is only applied to melting curves.

**Counterion Release.** The dependence of  $T_m$  on the sodium ion concentration for each of the three duplexes is shown in the inset of Figure 3. An increase in salt concentration results in a typical increase in the overall stability of the duplexes. From a linear regression analysis of the  $T_m$  vs the log  $[\text{Na}^+]$  plots, slopes ranging from 16 to 19 °C were obtained (Table 2). It has been shown that the values of these slopes are proportional to the difference in the number of bound counterions in the single-stranded and double-stranded states,<sup>34</sup>  $\Delta n_{\text{Na}^+}$ , according to the equation, which assumes a similar type of counterion binding to each state:

$$dT_m/d \ln [\text{Na}^+] = 0.9(RT_m^2/\Delta H_{\text{cal}})\Delta n_{\text{Na}^+} \quad (2)$$

where  $\Delta n_{\text{Na}^+} = n_{\text{Na}^+}(\text{ds}) - n_{\text{Na}^+}(\text{ss})$ , and 0.9 is a proportionality factor for converting mean ionic activities to ionic concentrations. The values of  $\Delta n_{\text{Na}^+}$ , as well as the variables from which these values were calculated, are listed in Table 2. The values of  $\Delta n_{\text{Na}^+}$  thus obtained range from 0.13 to 0.15 per phosphate residue. As expected, these values are somewhat lower than the value of 0.17 obtained for high molecular weight DNA, which is characteristic of ion-binding processes that take place within short DNA duplexes of this length with and without lesions.<sup>35</sup> Relative to the unmodified duplex, the counterion release parameters of the modified duplexes is similar in value. However, the counterion release parameters among the modified duplexes is different, corresponding perhaps to structural perturbations, as discussed in a later section.

**Standard Thermodynamic Profiles of Duplex Formation.** In order to directly compare our thermodynamic results obtained

(32) Rentzeperis, D.; Kupke, D. W.; Marky, L. A. *Biopolymers* **1993**, *33*, 117.

(33) Rentzeperis, D.; Rippe, K.; Jovin, T. M.; Marky, L. A. *J. Am. Chem. Soc.* **1992**, *114*, 5926.

(34) Record, T. M., Jr.; Anderson, C. F.; Lohman, T. M. *Q. Rev. Biophys.* **1978**, *11*, 103.

(35) Zieba, K.; Chu, T. M.; Kupke, D. W.; Marky, L. A. *Biochemistry* **1991**, *30*, 8018.

**Table 2.** Standard Thermodynamic Profiles for the Helix–Coil Transition of DNA Duplexes

duplex	UV melts		differential scanning calorimetry <sup>a</sup>						
	$\Delta H_{\text{shape}}$ (kcal/mol)	$\Delta H_{\text{vH}}$ (kcal/mol)	$T_m$ (°C)	$\Delta H_{\text{vH}}$ (kcal/mol)	$\Delta H_{\text{cal}}$ (kcal/mol)	$T\Delta S_{\text{cal}}$ (kcal/mol)	$\Delta G_{\text{cal}}$ (kcal/mol)	$dT_m/d$ $\log[\text{Na}^+]$ (°C)	$\Delta n_{\text{Na}^+}$ (per Pi)
unmodified	96(±15)	97(±15)	62.6(±0.5)	90(±9)	80.1(±3)	69.9(±2)	10.2(±0.4)	16.2(±0.8)	0.14(±0.01)
(-)-BPDE	82(±13)	74(±11)	57.7(±0.5)	73(±7)	72.7(±3)	64.4(±2)	8.3(±0.4)	19.1(±0.8)	0.15(±0.01)
(+)-BPDE	66(±10)	79(±12)	54.4(±0.5)	69(±7)	63.5(±3)	56.9(±2)	6.6(±0.3)	18.9(±0.8)	0.13(±0.01)

<sup>a</sup> Values were taken in 20 mM NaPi buffer containing 0.1 M NaCl at pH 7.0. The transition enthalpies were obtained as follows:  $\Delta H_{\text{shape}}$  from the shape of optical melts;  $\Delta H_{\text{vH}}$  from the slopes of  $1/T_m$  vs  $\ln C_T/4$  plots; the calorimetric  $\Delta H_{\text{vH}}$  from the shape of DSC curves; and  $\Delta H_{\text{cal}}$  from the area of the DSC curves. All the thermodynamic parameters are per mole of total duplex. The  $T_m$  values correspond to a strand concentration of 0.5 mM.

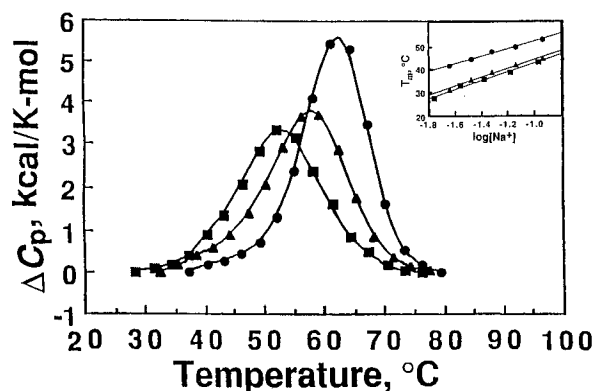


**Figure 3.** Differential scanning calorimetry curves for each duplex in 20 mM NaPi buffer containing 0.1 M NaCl at pH 7. The area under these curves corresponds to the transition enthalpy of each oligomer duplex: unmodified duplex (●), (-)-BPDE (▲), (+)-BPDE (■). The concentration in single strands was 500  $\mu\text{M}$  for the first two duplexes and 350  $\mu\text{M}$  for the (+)-BPDE duplex. Inset: Salt dependence of the transition temperature for each oligomer duplex, at a fixed strand concentration of  $\sim 6 \mu\text{M}$ , in same buffer and adjusted to the required NaCl concentration.

in melting experiments of each duplex, we present tabulated values of  $\Delta H_{\text{cal}}$ ,  $\Delta G_{\text{cal}}$ , and  $T\Delta S_{\text{cal}}$  in Table 2. All values have been extrapolated to the common temperature of 20 °C, the temperature at which the  $\Delta V$  and  $\Delta H_{\text{ITC}}$  measurements were made. The  $\Delta S_{\text{cal}}$  function was obtained in DSC experiments from the area under the curve of  $\Delta C_p/T$  vs  $T$ , and  $\Delta G_{\text{cal}}$  was calculated from the standard Gibbs equation at 20 °C. Overall, in all three cases, the free energies of formation are negative; these favorable free energy changes result from partial compensation of favorable changes in enthalpy and unfavorable entropy changes. The significant observation is that, relative to the unmodified duplex, the decrease in stability, by 4.9 and 8.2 °C, of the (-)-BPDE and (+)-BPDE duplexes, respectively, corresponds to unfavorable free energy changes of 1.9 and 3.6 kcal mol<sup>-1</sup>, respectively. These differential free energy changes reflect the loss of the heats of formation which are not quite compensated by favorable changes in the entropy terms (Table 2).

**Corrected Thermodynamic Parameters for the Formation of Duplexes at 20 °C.** The similarity of the enthalpies ( $\Delta H_{\text{ITC}} = \Delta H_{\text{cal}}$ ) for the formation of the unmodified duplex at 20 °C indicates a negligible contribution from base-stacking interaction of the unmodified single strands, while the lower  $\Delta H_{\text{ITC}}$  values for the BPDE–DNA duplexes (by 33–35 kcal/mol) show the expected endothermic contribution due to a weakening of stacking interactions in the modified single strands. Therefore, for a proper comparison with the isothermal heat and volume measurements, the  $\Delta G_{\text{cal}}$  and  $\Delta n_{\text{Na}^+}$  terms have been corrected<sup>36</sup> by the enthalpy factor  $\Delta H_{\text{ITC}}/\Delta H_{\text{cal}}$  to yield the thermodynamic profiles of Table 3. These corrected terms would therefore

**Table 3.** Complete Thermodynamic Characterization for the Formation of DNA Duplexes at 20 °C<sup>a</sup>

duplex	$\Delta G$ (kcal/mol)	$\Delta H_{\text{ITC}}$ (kcal/mol)	$T\Delta S$ (kcal/mol)	$\Delta n_{\text{Na}^+}$ (per duplex)	$\Delta V$ (mL/mol)
unmodified	-10.4(±0.6)	-82(±3)	-72(±3)	2.9(±0.2)	-144(±10)
(-)-BPDE	-5.4(±0.6)	-47(±2)	-42(±3)	2.0(±0.2)	-136(±11)
(+)-BPDE	-5.1(±0.6)	-49(±2)	-44(±3)	2.1(±0.2)	-209(±14)

<sup>a</sup> The  $\Delta G$  (from the corresponding DSC parameters) and  $\Delta n_{\text{Na}^+}$  values have been corrected by the factor  $\Delta H_{\text{ITC}}/\Delta H_{\text{cal}}$ , which includes the contribution of single-strand base-stacking interactions at 20 °C.

include the increased contribution of single-stranded base-stacking interactions at 20 °C. The overall favorable free energy terms of duplex formation in each case result in the characteristic partial compensation of exothermic enthalpies with unfavorable entropies, the latter term corresponding primarily to the uptake of both counterions and water molecules. The lower stability and lower enthalpic contribution of the BPDE–DNA duplexes, relative to the unmodified duplex, may be explained in terms of differences in base-pair stacking, hydrogen bonding, and overall hydration due to exposure of hydrophobic moieties to the solvent.

## Discussion

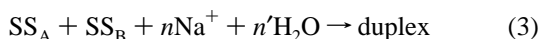
**Solution Structure of the (-)-BPDE- and (+)-BPDE Duplexes.** In order to correlate our thermodynamic parameters with the molecular interactions observed in the solution structure of the modified duplexes, we will briefly summarize studies of the solution structure of the (-)-BPDE duplex and the (+)-BPDE duplex obtained from NMR experiments.<sup>16,17</sup> In both structures, the aromatic pyrenyl ring systems are situated in the minor grooves of duplex DNA. This kind of positioning of the adducts results in a widening of the minor groove with the interstrand phosphate to phosphate distance increasing from 4.0 Å at each of the ends of the duplex to 8.1 Å at the adduct site. One face of the pyrenyl residue has an extensive number of van der Waals contacts with the sugar phosphate backbone of the complementary strand while the other face is exposed to solvent. In spite of the number of molecular contacts of the adduct and the duplex, the duplex is minimally distorted and the (BPDE)–dG•dC base pair maintains the Watson Crick base pairing with all of the hydrogen bonds intact. Although the pyrenyl residues in both the (+)-BPDE and (-)-BPDE duplexes are situated in the minor groove, the NMR experiments show definitively that there is a remarkable difference in the adduct orientations which is a result of the chirality of the two BPDE enantiomers;<sup>16,17</sup> in the case of the (-)-BPDE duplex, the adduct is oriented toward the 3' end of the modified strand, while in the (+)-BPDE duplex the adduct is oriented toward the 5' end of the modified strand. These adduct orientations were found earlier by energy-minimization searches of the potential energy

(36) Rentzeperis, D.; Kupke, D. W.; Marky, L. A. *Biochemistry* **1994**, *33*, 9588.

surface using the program DUPLEX;<sup>37</sup> however, it was not possible to conclude that the experimentally observed adduct orientation<sup>17</sup> was indeed the lowest energy conformer since a major groove adduct with a similar energy was also found.<sup>37</sup> Very recently, Fountain and Krugh characterized the solution structure of the (+)-BPDE–dG adduct<sup>38</sup> in a 11-mer duplex, where the main structural features are similar to those observed earlier,<sup>16</sup> but these authors reported the existence of more than one conformation for the bound adduct, due to differences in DNA sequence (the modified dG·dC base pair is actually flanked by (5' to 3') dT·dA and dC·dG base pairs).

There is another structural feature that distinguishes the (–)-BPDE and (+)-BPDE duplexes, at least when the modified guanine residues are flanked by T<sup>23a</sup> or G<sup>23b</sup> residues on both sides. In both cases the electrophoretic mobilities of the (+)-BPDE duplexes with trans-adduct stereochemistry were significantly slower than the mobilities of the *trans*-(–)-BPDE duplexes, suggesting that there is a greater degree of bending at the site of the lesion in the case of the (+)-BPDE duplex. These results are consistent with flow linear dichroism studies which show that (+)-BPDE covalently modified native DNA is more flexible than (–)-BPDE modified DNA;<sup>23a,39,40</sup> this increased flexibility gives rise to a shorter apparent persistence length in the case of the (+)-BPDE–DNA adducts.<sup>23a,41</sup>

**Complete Thermodynamic Profiles for the Formation of Each Duplex at 20 °C.** In order to discuss the observed thermodynamic parameters in terms of molecular and structural parameters, it is useful to cast the formation of a DNA duplex from two complementary single strands (SS<sub>A</sub> and SS<sub>B</sub>) into the following general form:



All of the thermodynamic parameters reported in Table 3 at 20 °C refer to the above reaction. Each single strand and each duplex has associated with it a certain number of sodium ions and bound water molecules. Formation of duplexes from the two single strands may be accompanied by changes in these parameters.

The overall free energy of formation of a DNA duplex includes the following contributions: (1) loss of entropy due to the bimolecular association of two strands; (2) loss of entropy due to the symmetry of the sequence (a combinatorial factor due to the complementarity of the two oligonucleotides), both terms contributing unfavorable free energy terms; (3) a favorable free energy term due to base stacking interactions; and (4) a free energy term associated with the hydrophobic BPDE residue. The first two terms are identical for the unmodified and the two BPDE-modified DNA sequences. The third term should be not significantly different either, because the NMR data suggest that the basic hydrogen bonding and base stacking parameters are similar in all three duplexes except that there is a widening of the minor groove in the immediate vicinity of the BPDE residues.<sup>16,17</sup> The observed differences in the free energy terms should thus depend primarily on the interactions and structures of the BPDE moieties in the minor groove of the (+)- and (–)-BPDE duplexes.

The observed enthalpies of duplex formation are different and comprise exothermic contributions from base-pair stacking

(37) Singh, S. S.; Hingerty, B. E.; Singh, U. C.; Greenberg, J. P.; Geacintov, N. E.; Broyde, S. *Cancer Res.* **1991**, *51*, 3482.

(38) Fountain, M. A.; Krugh, T. R. *Biochemistry* **1995**, *34*, 3152.

(39) Eriksson, M.; Nordin, B.; Jernström, B.; Grädslund, A. *Biochemistry* **1988**, *27*, 1213.

(40) Roche, C. J.; Geacintov, N. E.; Ibanez, V.; Harvey, R. G. *Biophys. Chem.* **1989**, *33*, 277.

(41) Nörden, B.; Kubista, M.; Kurucsev, T. *Q. Rev. Biophys.* **1992**, *25*, 51.

interactions, hydrogen-bonding, van der Waals interactions, and endothermic contributions due to increased hydration and base stacking of the single strands. The inclusion of BPDE in the modified duplexes decreases the exothermicity of the enthalpy by 35 and 33 kcal mol<sup>–1</sup> for the (–)-BPDE and (+)-BPDE duplexes, respectively (Tables 2 and 3). This can be attributed to the widening in the minor groove;<sup>17</sup> in addition, the (+)-BPDE duplex is bent and more flexible at the adduct site. Several possibilities can explain these enthalpy differences: (i) the widening of the minor groove could conceivably result in a net loss of optimum base-pair stacking interactions at the adduct sites, affecting up to three base-pair stacks, with no loss of hydrogen bonding; (ii) the placement of a molecule in the minor groove of B-DNA will result in the release of electrostricted water, an endothermic contribution<sup>35,42</sup> that may be similar with both modified duplexes; (iii) the similar area covered by both adducts will result in similar van der Waals contributions, with the exception of the specific atomic groups of BPDE that are exposed to solvent that would contribute exothermically due to a differential hydrophobic hydration;<sup>35</sup> and (iv) the bent or more flexible structure of the (+)-BPDE duplex could account for the larger enthalpy difference due to the higher ordering of hydrophobically bound water.<sup>35</sup> The endothermic contribution of single-strand stacking of the complementary strand can be assumed to be similar for all three duplexes and substantially different for the two modified strands.

The overall entropy change is equal to the sum of the following contributions: the  $\Delta S_{\text{mol}}$  (the loss of entropy due to a bimolecular association reaction) and  $\Delta S_{\text{sym}}$  (the loss in entropy due to the complementary nature of the oligomers). These two contributions are identical for all three duplexes.  $\Delta S_{\text{conf}}$  (changes in the oligomer configuration in going from single strand to duplex) is somewhat less unfavorable for the modified duplexes because of their more rigid structures;  $\Delta S_{\text{ion}}$  (uptake or release of counterions) is marginally similar for all three duplexes; and  $\Delta S_{\text{hyd}}$  (uptake of water molecules) is similar for the unmodified and (–)-BPDE duplexes, but is substantially different for the (+)-BPDE duplex according to our  $\Delta V$  measurements which correlates with the degree of reordering of water. This may be inconsistent with the lower unfavorable entropy term obtained in calorimetric melting experiments of the (+)-BPDE duplex (Table 2). However, the energy contribution of the  $\Delta S_{\text{hyd}}$  term in the melting of a nucleic acid duplex is usually small and is easily compensated with the increase in temperature.

The volume change accompanying the formation of a nucleic acid duplex is interpreted to reflect changes in the electrostriction and/or hydrophobicity of water dipoles, which are immobilized by each of the participating species. These two effects tend to compensate each other in this type of reaction. For the comparison of the thermodynamic profiles of the duplexes at 20 °C (see next section) we are assuming that the modified strands have a similar contribution to the  $\Delta V$ ; this may be true because these two strands have a similar chemical composition.

#### Differential Thermodynamic Profiles Indicate a Higher Ordering of Structural Water for the (+)-BPDE Duplex.

Comparison of the isothermal thermodynamic parameters for the formation of each of the BPDE–DNA duplexes with those of the unmodified duplexes yields a  $\Delta\Delta G$  ( $\Delta G(\text{modified}) - \Delta G(\text{unmodified})$ ) of +5 kcal/mol of duplex. This results from a partial compensation of an unfavorable  $\Delta\Delta H_{\text{TTC}}$  of 34 kcal/mol of duplex with a favorable  $\Delta(T\Delta S)$  of 29 kcal/mol of duplex, and a similar differential counterion release,  $\Delta\Delta n_{\text{Na}^+}$  of  $\sim 0.8$  mol of Na<sup>+</sup> per mol of duplex. However, the  $\Delta\Delta V$

(42) Gasan, A. J.; Maleev, V. Ya.; Semenov, M. A. *Stud. Biophys.* **1990**, *136*, 171.

terms show a marginally positive value of +8 mL per mol of duplex for the (–)-BPDE duplex, but a clearly negative value of –65 mL per mol of duplex for the (+)-BPDE duplex. The similar signs of the differential enthalpy–entropy compensation and  $\Delta\Delta V$  for the (–)-*trans*-BPDE duplexes are characteristic of processes that are driven by differential hydration due to electrostriction,<sup>35–36,43</sup> while the opposite signs of the differential enthalpy–entropy compensation and the  $\Delta\Delta V$  for the (+)-*trans*-BPDE duplexes are characteristic of processes that are driven by a differential structural hydration as has been described previously.<sup>35</sup> This strongly suggests a greater exposure of hydrophobic residues to the aqueous solvent environment in the case of the (+)-BPDE–DNA than in the case of the (–)-BPDE–DNA duplexes.

**Comparison with Previous Thermodynamic Results of Related Systems. (a) Duplexes Containing Adducts.** There are relatively few additional studies of the thermodynamic characteristics of oligonucleotides covalently modified with bulky hydrophobic aromatic polycyclic aromatic hydrophobic residues. Using UV spectroscopic techniques, Cosman et al.<sup>15a,44</sup> have studied the melting profiles of analogous (+)- and (–)-BPDE–N<sup>2</sup>-dG *trans*-addition product in the sequence 5'-CACATGTACAC-3' complexed with its complementary strand 5'-GTGTCAGTGT-3'; at a 10  $\mu$ M concentration of modified strands in the duplex form, the  $T_m$  values were 45.2, 32.1, and 27.9 °C for unmodified and (+)-BPDE- and (–)-BPDE-modified duplexes, respectively, under the same buffer conditions as used in this work.<sup>44</sup> Consistent with the results reported here, both *trans*-BPDE-modified duplexes are destabilized relative to the unmodified double-stranded oligonucleotide; however, the (–)-*trans* adduct exhibits a somewhat lower melting point than the (+)-*trans*-BPDE adduct, which is different from the relative ordering of the  $T_m$ 's obtained by us (Table 3) and by Ya<sup>15b</sup> for our oligonucleotide sequence, in which the BPDE-modified G is flanked by two C's rather than by two T's. The extent of destabilization of the duplexes thus depends not only on the configuration of the substituents about the four chiral carbon centers in the covalently bound BPDE residues but also on the bases flanking the lesion, as well as on the sequence context of the complementary strand.<sup>15b</sup>

Stezowski et al.<sup>45</sup> have studied the melting temperatures of three different oligonucleotides 7, 9, and 15 bases long in which a 7-methylene-12-methylbenzo[*a*]anthracenyl moiety is covalently attached to the N<sup>6</sup>-position of an adenosine; this bulky PAH moiety is believed to reside at an external binding site, probably in the major groove. No duplexes were formed with the complementary strand in the case of the 7-mer, and the duplexes resulting from the alkylated 9-mer and 15-mer were destabilized by the polycyclic aromatic residues. Casale and McLaughlin<sup>46</sup> have studied a covalently modified 13-mer oligonucleotide duplex d(GTTATCCG\*CTCAC)/d(GTGAGCG-GATAAC) containing an N<sup>2</sup>-(anthracen-9-ylmethyl) moiety at the starred guanosine residue, most likely situated in the minor groove. The melting data were consistent with a two-state model, and the modified duplex was destabilized by 6 °C due to changes in the entropy rather than enthalpy of melting. In contrast, Telser et al.<sup>47,48</sup> reported that the attachment of one or two pyrenyl residues to thymidine bases via an aliphatic 8–10 atom linker results in a stabilization of a double-stranded octamer, possible because of an intercalative insertion of the pyrenyl residues between adjacent base pairs.

(43) Marky, L. A.; Kupke, D. W. *Biochemistry* **1989**, *28*, 9982.

(44) Cosman, M. Ph.D. Dissertation, New York University, 1991.

(45) Stezowski, J. J.; Loos-Guba, G.; Schvnwldler, K. H.; Straub, A.; Glusker, J. P. *J. Biomol. Struct., Dynamics* **1987**, *5*, 615.

(46) Casale, R.; McLaughlin, L. W. *J. Am. Chem. Soc.* **1990**, *112*, 5264.

(47) Telser, J.; Cruickshank, K. A.; Morrison, L. E.; Netzel, T. L. *J. Am. Chem. Soc.* **1989**, *111*, 6966.

**(b) Duplexes Containing Extrahelical Bulges.** The helix–coil transition of duplexes containing imperfections, such as bulge bases and base-pair mismatches, is accompanied by  $T_m$ 's and transition enthalpies that are lower in magnitude than those of their fully paired parent duplexes. The melting behavior of our modified duplexes can be viewed as being similar to that of duplexes containing extrahelical bulges, which show intact base pairing and base-pair stacking interactions with the extrahelical bulge base phasing the major groove of DNA and partially exposed to solvent;<sup>49</sup> depending on the nature of the bulge base, these duplexes are bent. Zieba et al.<sup>35</sup> reported thermodynamic data of such systems in which the reduced stability of the duplexes containing the bulged bases adenine and thymine corresponded to reduced unfavorable enthalpic interactions with an increase in the uptake of both counterions and water molecules; a higher amount of structurally (hydrophobic) bound water was reported with the duplex having the A bulge. Therefore, we proposed that the enhanced hydration of the (+)-BPDE–DNA duplex as compared to the (–)-BPDE–DNA duplex can be correlated with the observed pronounced local bend of this duplex.<sup>22</sup> Structural distortions induced by the binding of bulky mutagens and carcinogens to DNA, and differences in the extent of hydrations of these hydrophobic covalent bound ligands, may play important roles in the interactions of the damaged DNA with regulatory, repair, replication, and other proteins.

## Conclusions

Complete thermodynamic profiles ( $\Delta H$ ,  $\Delta V$ ,  $\Delta G$ ,  $\Delta S$ , and  $\Delta n_{Na^+}$ ) for the formation of each duplex were determined at 20 °C. Relative to the unmodified duplex, the (+)-BPDE–DNA and (–)-BPDE–DNA duplexes are characterized by lower thermal stabilities that are primarily due to lower exothermic enthalpies of formation of the BPDE-modified duplexes. The formation of each of the three duplexes is accompanied by unfavorable entropies of formation, which is attributable to an uptake of both counterions and water molecules. The  $\Delta V$  value is only marginally smaller for the (–)-BPDE–DNA than for the unmodified duplex; however, the uptake of water is significantly greater in the case of the (+)-BPDE duplex than for the other two types of duplexes. Analysis of the thermodynamic data, together with nearly identical changes in bound counterions ( $\Delta n_{Na^+}$ ), suggests that the larger  $\Delta V$  value for the formation of the (+)-BPDE–DNA duplex than for the (–)-BPDE–DNA duplex is due to a difference in the hydration of the BPDE residues that are exposed to solvent in the minor grooves of B-DNA. These results strongly suggest that the formation of the (+)-BPDE duplex results in an additional immobilization of water molecules; the bent conformation at the lesion site of the (+)-BPDE–DNA duplex<sup>23</sup> apparently gives rise to greater exposure of the hydrophobic groups of this covalent bound BPDE moiety to the aqueous solvent.

**Acknowledgment.** This work was supported by NIH Grants GM42223 (L.A.M.) and GM34938 (D.W.K.) and Department of Energy Office of Health and Environmental Research Grant DE-86ER06045 (N.E.G.). The synthesis of the unmodified and modified oligonucleotides was supported by the NIH/NCI, Grant CA20851 (N.E.G.).

JA9538703

(48) Telser, J.; Cruickshank, K. A.; Morrison, L. E.; Netzel, T. L.; Chan, C.-K. *J. Am. Chem. Soc.* **1989**, *111*, 7226.

(49) Le Blanc, D. A.; Morden, K. M. *Biochemistry* **1991**, *31*, 4042.